Electronic Supplementary Material (ESI) for CrystEngComm.

Porous nickel and cobalt hexanuclear ring-like clusters built from two different kind of calixarene ligands - new molecular traps for small volatile molecules

Mariia V. Kniazeva,[a] Alexander S. Ovsyannikov,[a]* Beata Nowicka,[b] Nathalie Kyritsakas,[c] Aida I. Samigullina,[a] Aidar T. Gubaidullin,[a] Daut R. Islamov,[d] Pavel V. Dorovatovskii,[e] Elena V. Popova,[a] Sofiya R. Kleshnina,[a] Svetlana E. Solovieva,[b] Igor S. Antipin,[b] Sylvie Ferlay[c]*

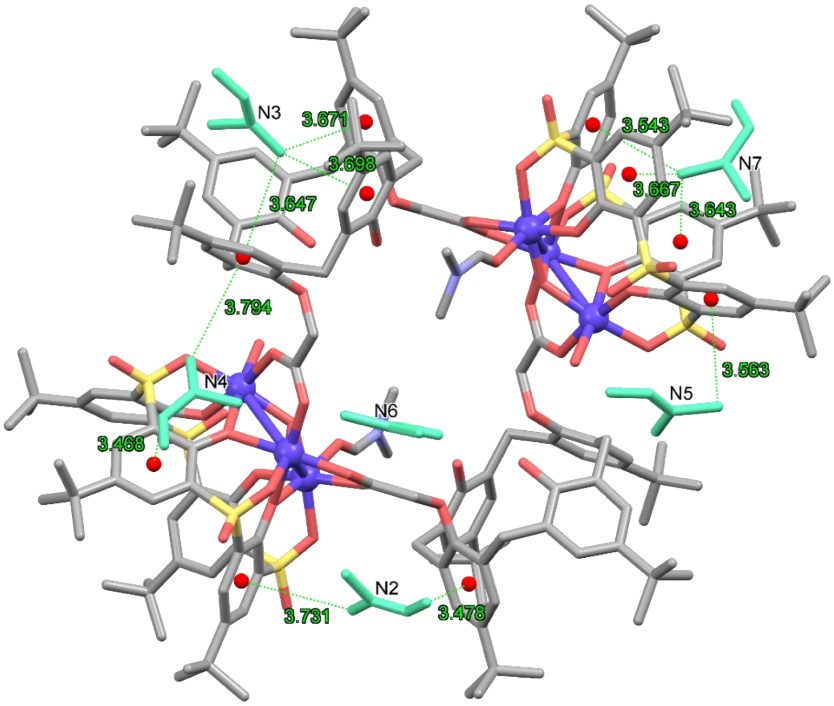

Figure S1. C-H-π interactions between crystallization DMF molecules (light green) and calixarene aromatic rings in (**2**-2H)$_2$**3**$_2$Co$_6$. No interactions are observed for the molecules located in the internal channels (N6).

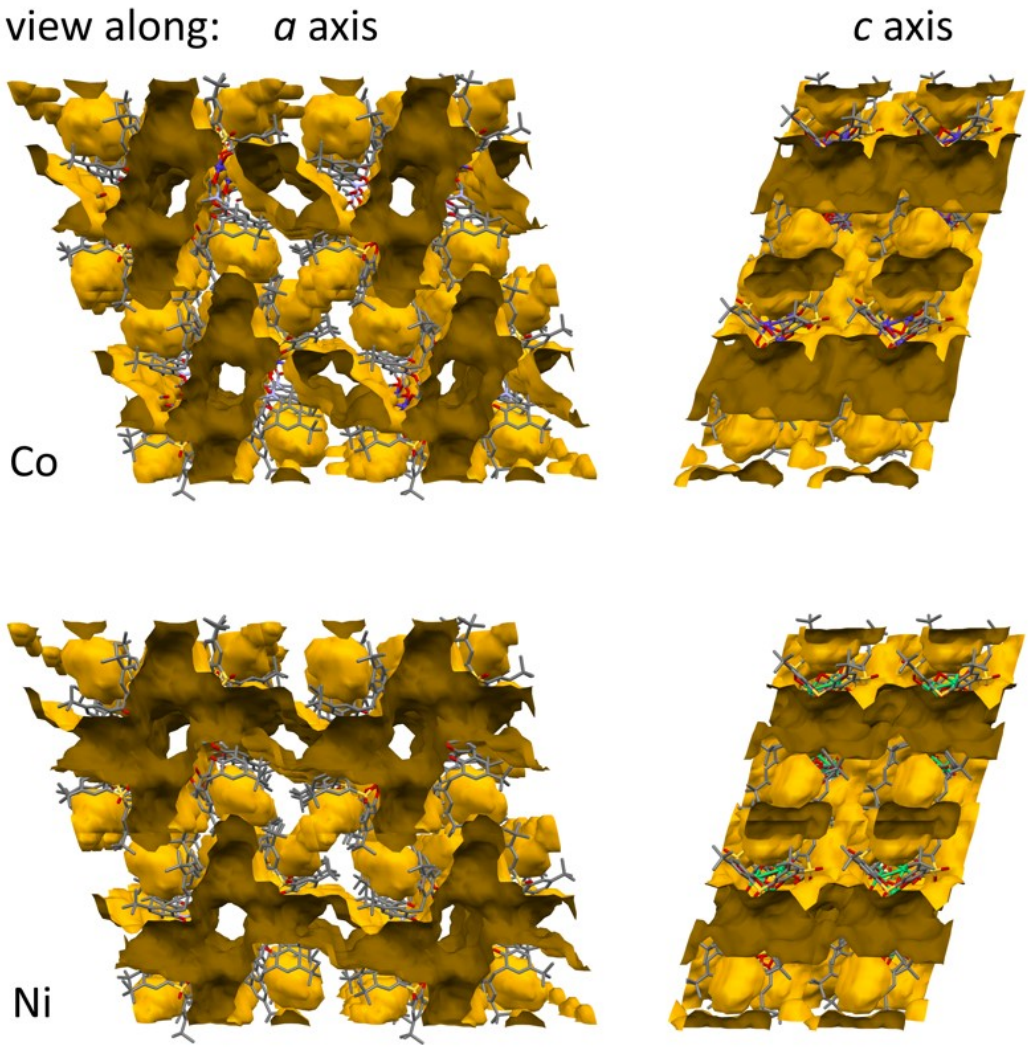

Figure S2. Visualization of the solvent-accessible voids fo (**2**-2H)$_2$**3**$_2$Co$_6$ and (**2**-2H)$_2$**3**$_2$Ni$_6$. The view presents structure fragment of 2x2x2 unit cells. In the view along the *a*-axis (left) four internal channels are visible at the center of each cell, while the external channels are visible between the unit cells. The view along the *c*-axis (right) shows the intersection of the external channels and the separated capsules formed by calixarene cavities.

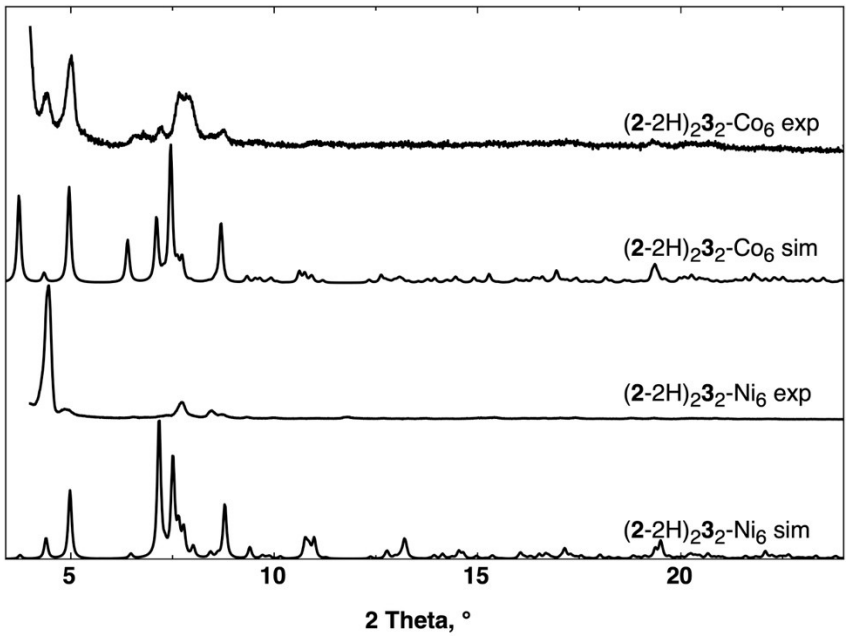

Figure S3. For air-dried (**2**-2H)$_2$**3**$_2$Co$_6$ and (**2**-2H)$_2$**3**$_2$Ni$_6$, comparison of the simulated and experimental powder X-Ray diffraction studies (PXRD) diagrams at a scan step size of 2° min-1.

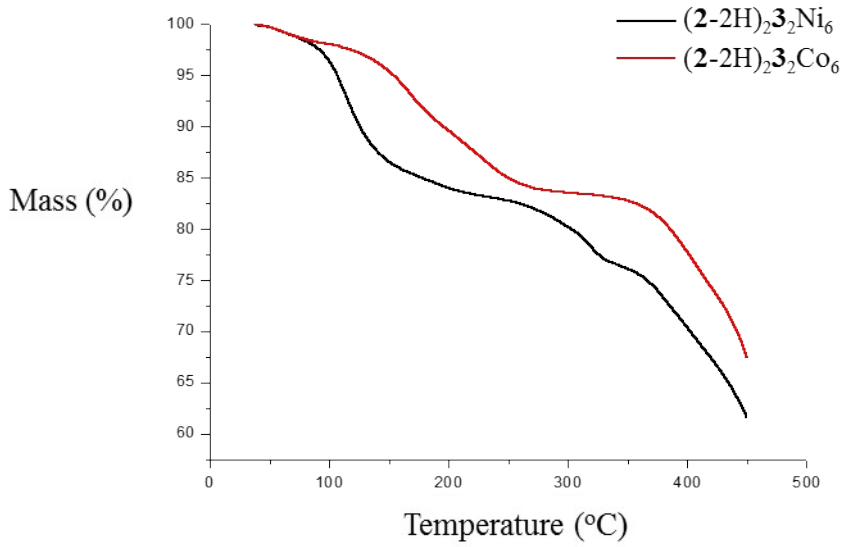

Figure S4. For (**2**-2H)$_2$**3**$_2$Co$_6$ and (**2**-2H)$_2$**3**$_2$Ni$_6$ TGA traces recorded between 36 - 450°C at a rate of 10°/mn.

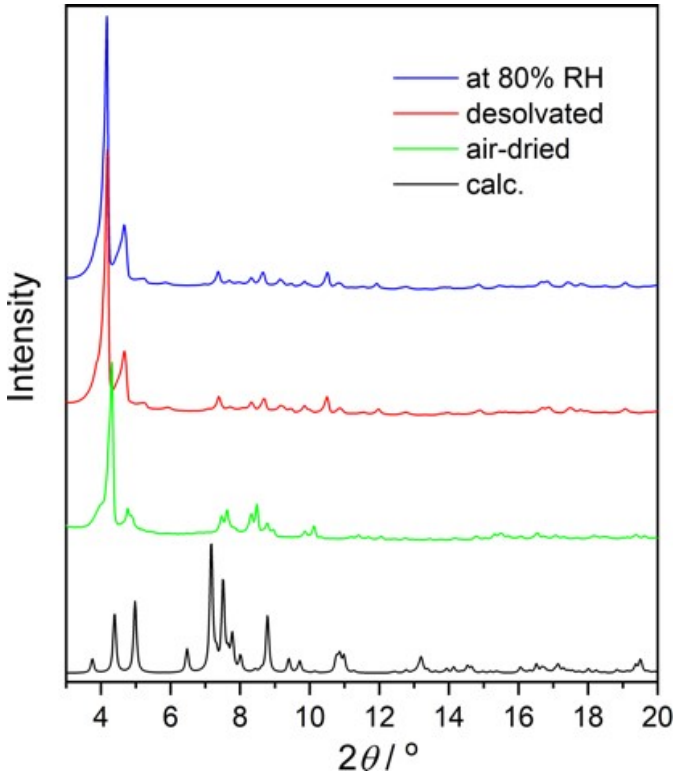

Figure S5. PXRD patterns for air-dried (green), totally desolvated (red) and hydrated (blue) samples of (**2**-2H)$_2$**3**$_2$Ni$_6$ compared to simulated one, showing anisotropic peak shifts due to lattice structural variations imposed by the structural adaptation to the guest molecules exchange.

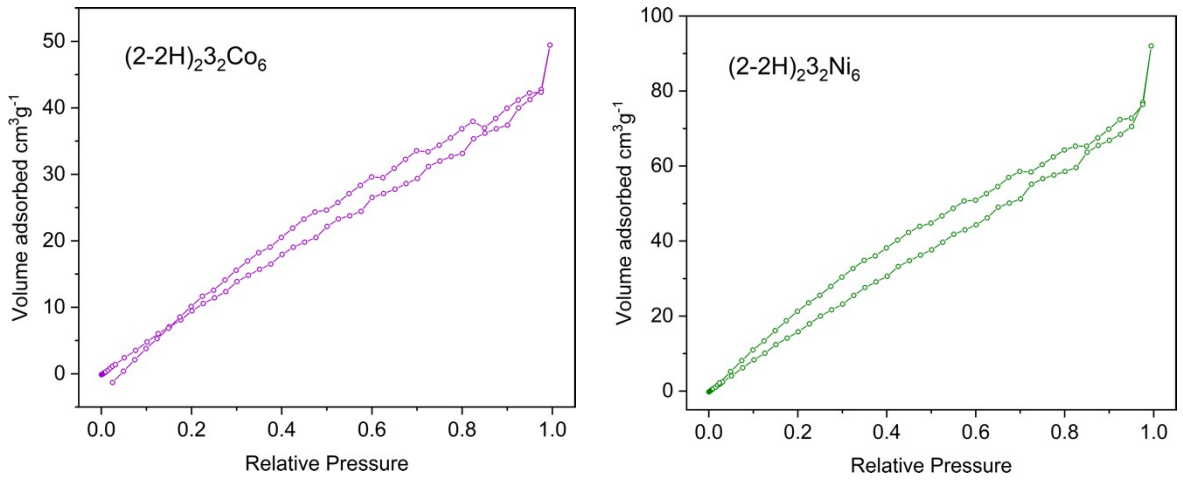

Figure S6. N_2 sorption isotherms at 77K for (**2**-2H)$_2$**3**$_2$Co$_6$ and (**2**-2H)$_2$**3**$_2$Ni$_6$.

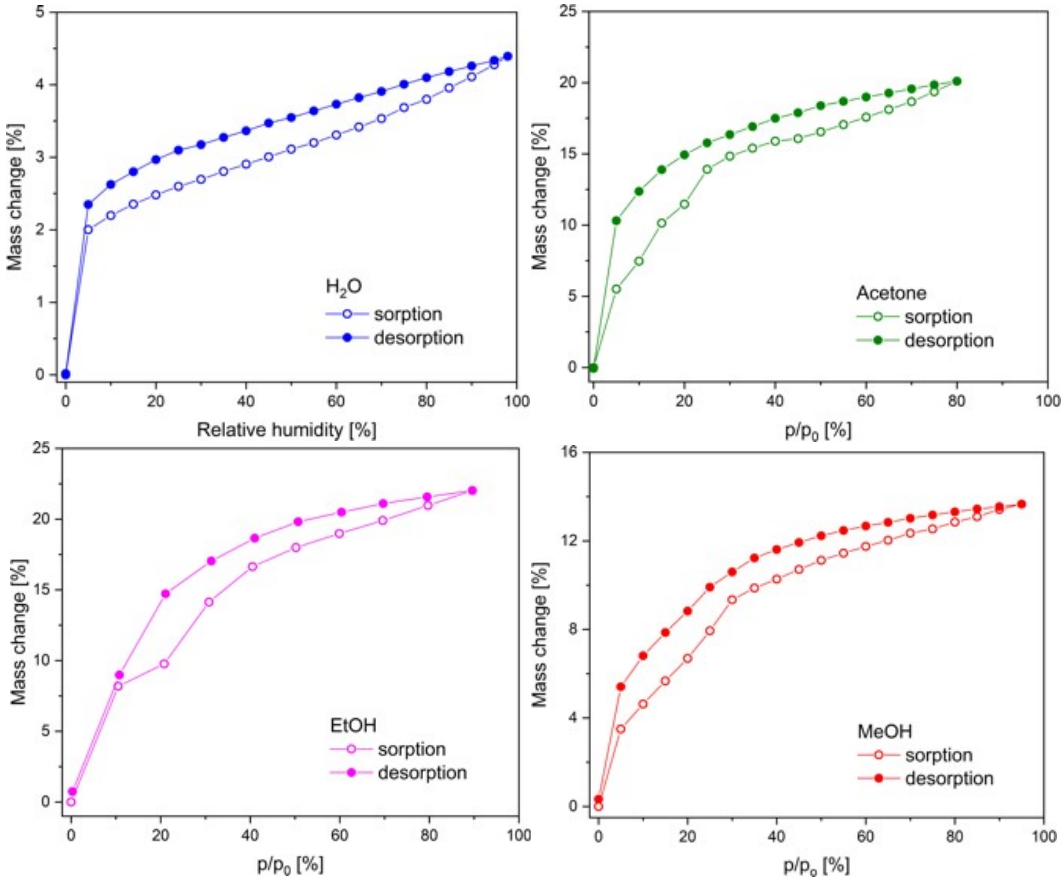

Figure S7. Sorption isotherms for (**2**-2H)$_2$**3**$_2$Ni$_6$ measured by the gravimetric dynamic vapor sorption method at 25°C in the p/p$_0$ range of a) 0-98% (H_2O), b) 0-80% ($CH_3C(O)CH_3$), c) 0-90% (EtOH), d) 0-95% (MeOH).

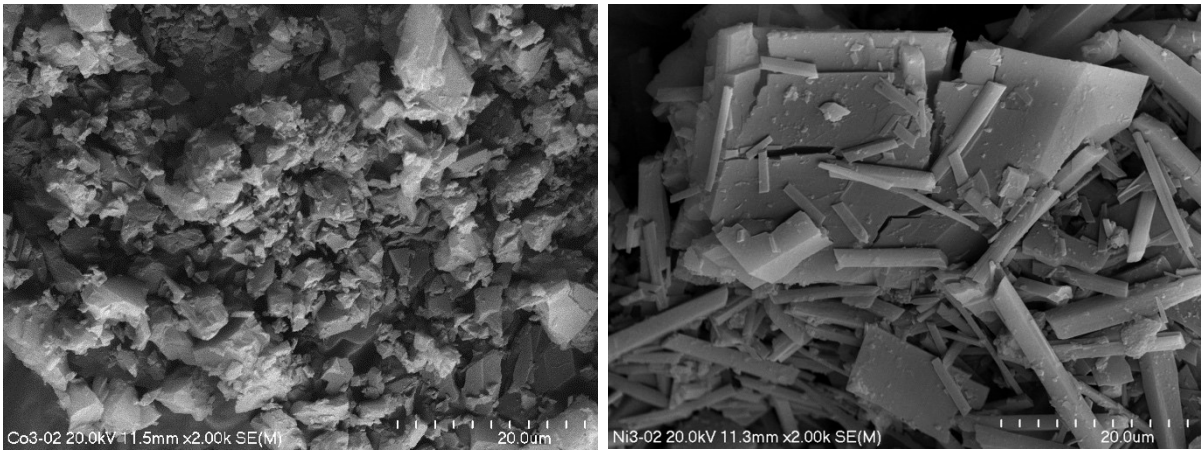

Figure S8. SEM images of the microcrystalline samples of (**2**-2H)$_2$**3**$_2$Co$_6$ (left) and (**2**-2H)$_2$**3**$_2$Ni$_6$ (right).

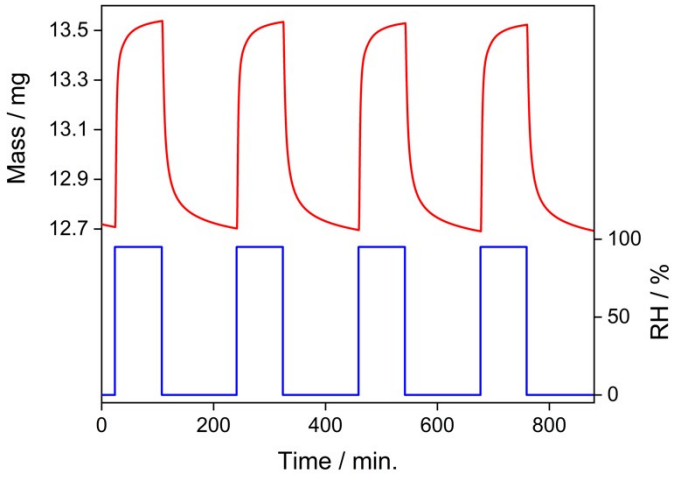

Figure S9. Repeated water sorption and desorption cycles for (**2**-2H)$_2$**3**$_2$Co$_6$.

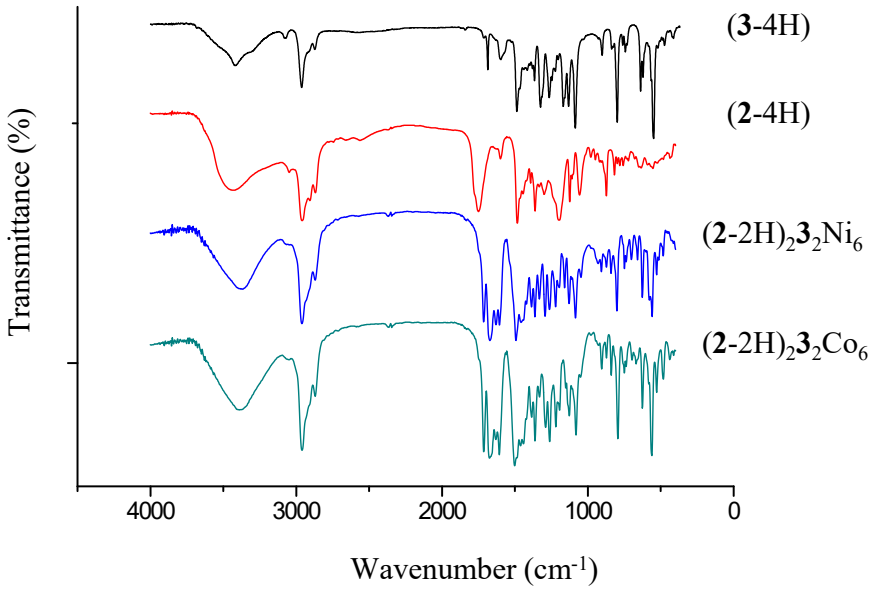

Figure S9. IR-spectrum of (**3**-4H), (**2**-4H), (**2**-2H)$_2$**3**$_2$Ni$_6$ and (**2**-2H)$_2$**3**$_2$Co$_6$.